Enabling complete conversion of CH_4 and CO_2 in dynamic coke-mediated dry reforming (DC-DRM) on Ni catalysts

Pinto, Donato; Hu, Lingjun; Urakawa, Atsushi

DOI
10.1016/j.cej.2023.145641

Publication date
2023

Document Version
Final published version

Published in
Chemical Engineering Journal

Chemical Engineering Journal 474 (2023) 145641

Contents lists available at ScienceDirect

Chemical Engineering Journal

journal homepage: www.elsevier.com/locate/cej

Enabling complete conversion of CH_4 and CO_2 in dynamic coke-mediated dry reforming (DC-DRM) on Ni catalysts

Donato Pinto [a,1], Lingjun Hu [a,b,1], Atsushi Urakawa [a,*]

[a] Catalysis Engineering, Department of Chemical Engineering, Delft University of Technology, Van der Maasweg 9, 2629 HZ Delft, The Netherlands
[b] Institute of Chemical Research of Catalonia (ICIQ), The Barcelona Institute of Science and Technology, Av. Països Catalans 16, 43007 Tarragona, Spain

ARTICLE INFO

Keywords:
CH_4 dry reforming
CO_2 conversion
Heterogeneous catalysis
Ni catalysts
Unsteady-state

ABSTRACT

Dynamic coke-mediated dry reforming of methane (DC-DRM) is an unsteady-state strategy to overcome the limitations of co-feed operation, including the fast deactivation of the catalysts and the loss of valuable H_2 in the reverse water gas-shift reaction. This paper proves the feasibility of DC-DRM on Ni-based catalytic systems, identifying suitable metal oxides supports and evaluating the role of metallic promoters. A La-promoted Ni/ZrO_2 catalyst exhibited excellent and stable catalytic performances at 800 °C approaching complete conversion of the CH_4 and CO_2 reactant pulses in the reaction loop, and separation of the H_2 and CO product streams. Adding the redox functionality of reducible oxides (TiO_2) in the catalyst support is demonstrated as a powerful tool to enable direct formation of syngas in the methane pulse with control on the H_2/CO ratio.

1. Introduction

Thanks to the abundant reserves of natural gas, its main component, methane, represents a readily available alternative to oil-based fossil fuels. In the last decades, dry reforming of methane (DRM, Reaction (1)) attracted great scientific and technological interests.[1,2] The reason is in the possibility of simultaneously convert methane and carbon dioxide to produce a syngas (CO + H_2).

$$CH_4 + CO_2 = 2H_2 + 2CO \qquad \Delta H^0_{298} = 247\ kJmol^{-1} \tag{1}$$

Compared to the conventional technologies for commercial syngas production involving steam or oxygen as oxidant (steam reforming of natural gas with large energy input as heat, autothermal reforming, partial oxidation), the direct utilisation of CO_2 as reforming agent of CH_4 in the DRM process can result in carbon footprint mitigation and potentially make it a 'greener' alternative.[3,4] Compared to steam reforming in particular, the energy requirements to provide high-temperature steam are cut down. Moreover, a syngas with lower H_2/CO ratio can be obtained as product, which is a more favourable feedstock, for example, to promote chain growth reactions in Fischer-Tropsch synthesis of hydrocarbons or for the direct synthesis of dimethyl ether.[5–7].

DRM is a strongly endothermic reaction, requiring high temperatures to activate the highly stable chemical bonds of both CH_4 and CO_2 molecules. Thermodynamic equilibrium analyses of CH_4 and CO_2 mixtures show that high conversions can be obtained only at very high temperatures (T > 800 °C).[8] In such conditions, the global reaction proceeds via two main routes involving the decomposition of methane (Reaction (2)) to form solid C and gaseous H_2, and the gasification of C by CO_2 to produce CO by the reverse Boudouard reaction (Reaction (3)). At the same time, the endothermic reverse water–gas shift (RWGS, Reaction (4)) can be activated. In this reaction route, the H_2 evolved from CH_4 decomposition is consumed by reacting with CO_2 from the feed. As a result, the syngas is enriched in CO, with H_2/CO ratio below 1, and contains undesired H_2O, demanding additional processing in order to meet the requirements of downstream operations, as methanol or hydrocarbon synthesis.

$$CH_4 = C + 2H_2 \qquad \Delta H^0_{298} = 74.9\ kJmol^{-1} \tag{2}$$

$$C + CO_2 = 2CO \qquad \Delta H^0_{298} = 172.4\ kJmol^{-1} \tag{3}$$

$$H_2 + CO_2 = H_2O + CO \qquad \Delta H^0_{298} = 41\ kJmol^{-1} \tag{4}$$

The extreme conditions required for achieving high conversions of CH_4 and CO_2 represent an hard proof for the catalyst materials. In fact, high temperatures usually translates into fast catalyst deactivation. The

* Corresponding author.
E-mail address: A.Urakawa@tudelft.nl (A. Urakawa).
[1] These authors have contributed equally.

https://doi.org/10.1016/j.cej.2023.145641
Received 23 April 2023; Received in revised form 12 August 2023; Accepted 23 August 2023
Available online 24 August 2023

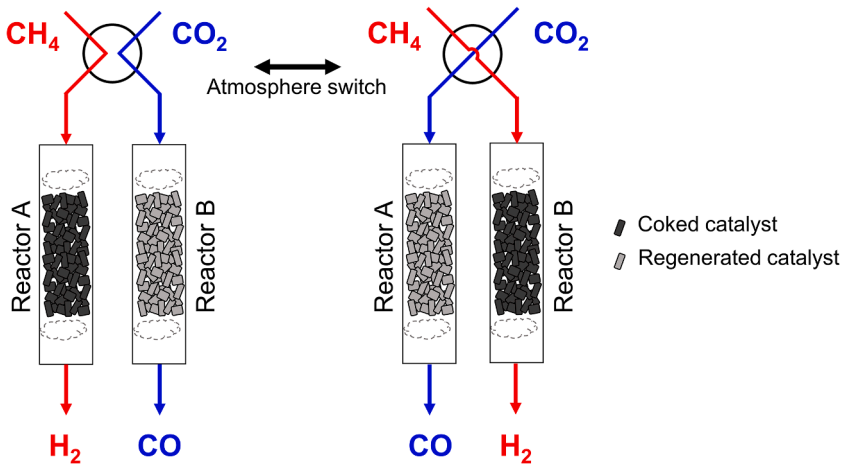

Scheme 1. Representation of Dynamic Coke-mediated Dry Reforming of Methane (DC-DRM) operated in alternating fixed bed reactors. For the purpose of this investigation, reactant feeds are alternated to a single fixed bed reactor and inert flushing phases (He) are interposed to eliminate possible influences to the catalytic results deriving from direct mixing of the reactants.

major causes of catalyst deactivation are sintering of the active metal and accumulation of stable carbon deposits, which can be accompanied by undesired pressure build-up in fixed bed reactors, abrupt changes in the thermal conductivity and catalyst fouling.[2,9] In presence of a catalyst, the formation of stable carbon deposits becomes unavoidable when big particle sizes are involved.[10] Metal oxides with high thermal stability are commonly employed as support materials for DRM catalysts. The effect of the support metal oxides on the DRM catalytic performances is frequently investigated.[11] Thanks to its high surface area, favouring the dispersion of the active metal phase, γ-Al_2O_3 is a common choice as DRM catalysts support, although phase transitions are observed at the high temperatures of reaction.[12,13] Good dispersion of the active metal can be achieved also on SiO_2, known for its inertness as support material.[14] The use of ZrO_2 as support guarantees high stability of the DRM performances, balancing between a good activity in CH_4 conversion and the higher reactivity of the carbon deposits towards CO_2.[15,16] Excellent activity in promoting DRM has been demonstrated over catalytic materials containing platinum-group metals (PGMs). Noble metal-based catalysts offer often outstanding performance in terms of reaction temperature and stability. Alternative catalytic systems containing more abundant transition metals as Fe, Co and Ni are also widely investigated. Compared to Co and Fe, the higher resistance of Ni towards oxidation makes it more attractive in the formulation of highly active DRM catalysts.[1,11,17,18].

The high rate of methane decomposition on Ni-based catalysts translates into fast coking and deactivation. In fact, CH_4 can be chemisorbed on Ni with direct cleavage of a C-H bond and stepwise dehydrogenation until deposition of a C atom. The C atoms can diffuse on/in the Ni particles so that carbon deposits grow in the form of whiskers with a Ni particle at the top. Thus the activity towards CH_4 decomposition is maintained while carbon deposits grow at a constant rate.[2] Partial passivation of the active Ni surface with sulfur was employed in SPARG process, sacrificing the overall activity to limit the growth of carbon deposits.[19] The use of promoters can be an effective strategy to reduce the deactivation of Ni-based catalysts. The addition of K is an example of an effective strategy to prevent carbon accumulation during DRM. [20] Increased dispersion and decrease in crystallite size can be achieved by using La as promoter, resulting in the enhancement of the DRM performance. [21] Bimetallic catalysts (e.g. Ni-Fe, Ni-Co) are recently investigated in order to mitigate the carbon deposition.[22–25] Combining Ni with traces of noble metals positively influences the activity while reducing the extent of coking.

Additional limitations to the exploitation of DRM derive from the intrinsic nature of conventional operational modes, which involve the co-feeding of the reactants leading to catalyst deactivation and difficulty in steady operation (*vide infra*). To overcome the limitations imposed by co-feed operation and the harsh reaction condition, a possibility is offered by unsteady-state processes, involving a paradigm change in the DRM operation mode. A first important benefit targeted by unsteady-state operation is feedstock and/or product separation, considering that separation is one of the most energy-intensive processes in chemical industry. An example is given by chemical looping operated processes, [26] which consist in the cyclical exposure of the catalytic material to the alternation of the separate gaseous reactants, commonly an oxidant and a reductant. Interconnected fluidised bed reactors, rotating reactors or alternating fixed bed reactors are required in order to expose the catalyst to the different atmospheres by either physically transporting the catalyst between the oxidising and the reducing reactors or switching the gaseous atmosphere of each reactor.[27] This operation mode has been successfully developed to improve the efficiency of catalytic combustion of hydrocarbon fuels [28,29].

In a similar fashion, chemical looping dry reforming of methane (CL-DRM) was proposed using oxygen-carrier catalytic materials that mediate between the reducing (CH_4) and oxidising (CO_2) reactant phases.[27,30–32] Najera et al.[30] proposed a CL-DRM process as an alternative chemical looping combustion of CH_4 which enables utilisation of CO_2 as oxidant (Reaction (5)). CH_4 is oxidised to CO_2 and H_2O (Reaction (6)) by reaction with the oxygen of the carrier catalytic material (metal oxide 'MO'). After that, the carrier material is re-oxidised in CO_2 (Reaction (7)), with simultaneous production of CO. In this process, CO is the only targeted product with no selectivity towards H_2, which is wasted during the total oxidation of CH_4 to CO_2 and H_2O by the oxygen carrier material.

$$CH_4 + 3CO_2 = 4CO + 2H_2O \quad (5)$$

$$CH_4 + 4MO = 4M + CO_2 + 2H_2O \quad (6)$$

$$4CO_2 + 4M = 4CO + 4MO \quad (7)$$

Sorption-enhanced DRM processes based on calcium looping are also proposed to enhance the conversion of CO_2.[33] With the aim of intensifying CO_2 utilisation, Buelens et al.[34] combined the reforming (Ni), redox (Fe) and CO_2 sorption (Ca) functionalities in the catalytic bed, defining a 'super-dry' reforming of CH_4. In this process, H_2 and CO deriving from CH_4 conversion are sacrificed to reduce the oxygen carrier material with formation of CO_2 and H_2O, a common trait of CL-DRM processes.[35] The presence of the CaO sorbent promotes *in situ* capture of CO_2 to form $CaCO_3$, while H_2O is removed from the reactor. Switching to an inert feed, regeneration of the CaO sorbent takes place

with release of CO, which is thus inherently separated from the H_2O byproduct.

Several limitations can be pointed out for the CL-DRM. From operational point of view, achieving chemical looping operation requires circulating fluidised bed with high catalyst circulation rates. Additionally, sintering and degradation of the oxygen carriers materials represents an additional source of catalyst deactivation. Moreover, the employment of oxygen carriers typically results in the formation of total oxidation products (i.e·H_2O and CO_2) and low yields of H_2 and CO.

In this work, we present an unsteady-state DRM operation able to provide high conversions of CH_4 and CO_2 and intrinsic separation of the feed and product streams, while targeting high H_2 and CO yield. Inherent separation of both reactant and product streams is achieved by periodic switching of the gas feed at the inlet of a fixed-bed reactor. The global DRM reaction is thus divided in two stages (Scheme 1), the CH_4 decomposition (Reaction (2)) and the C gasification by CO_2 (Reaction (3)). Contrarily to conventional DRM operation, the carbon deposits (coke) represent here the targeted intermediate between the H_2 generation from CH_4 and the CO formation from CO_2. Accordingly, we coin this process as a Dynamic Coke-mediated Dry Reforming of Methane (DC-DRM). In DC-DRM the catalytic system undergoes substantial transformations during each reactant pulse, transitioning from a coke-free state in the CO_2 pulse to a coke-saturated state at the end of the CH_4 pulse. The irreversible accumulation of carbon deposits is tackled by the cyclic alternation of short reducing and oxidising reactant pulses in DC-DRM. This approach is expected to limit the irreversible accumulation of carbon deposits, favouring their complete gasification in each operation cycle and thus extending the stability of the catalyst performance. Additionally, an intrinsic advantage of the unsteady-state operation is the elimination of RWGS (Reaction (4)) by precluding the mixing of the H_2 with the CO_2 feed. The result is a more valuable syngas, enriched in H_2, and the avoidance of undesired H_2O formation. In this perspective, it is decisive to select an optimal catalyst for DC-DRM operation able to provide fast decomposition of CH_4 with formation of carbon deposits that can be efficiently gasified in CO_2.

The work here presented proves the feasibility of DC-DRM operation and its potentiality towards full conversion of CO_2 and CH_4 reactant to CO and H_2, respectively. To this scope, Ni-based catalysts were synthesised and tested. The performance of different irreducible (SiO_2, ZrO_2, γ-Al_2O_3) and reducible (TiO_2) metal oxides supports was evaluated, together with the investigation of different metal promoters (La, Fe, K), with the aim of achieving full conversion of CH_4 and CO_2 in the catalytic cycle and providing stable operation in DC-DRM conditions.

2. Experimental

2.1. Catalyst synthesis

Aluminum oxide (γ-phase, Alfa Aesar, 255 $m^2\ g^{-1}$), silicon oxide (Alfa Aesar, surface area 261 $m^2\ g^{-1}$) zirconium oxide (Alfa Aesar, 90 $m^2\ g^{-1}$) and titanium dioxide (rutile, Alfa Aesar, >99.5%) were employed as support material. For the TiO_2-ZrO_2 mixed oxide, ZrO_2 powder was impregnated in inert (N_2) atmosphere with a titanium (IV) isopropoxide solution (Sigma Aldrich, 97%) to obtain a 20/80 wt% TiO_2/ZrO_2 composition (Ti/Zr molar ratio = 15/85). The catalyst was then dried at 80 °C overnight and calcined in air at 800 °C for 5 h. Ni was added by incipient wetness impregnation using nickel nitrate hexahydrate (Alfa Aesar, >98%) as precursors on the different supports to synthesise the Ni/Al_2O_3 (15/85 wt%, NA), Ni/SiO_2 (15/85 wt%, NS), Ni/ZrO_2 (15/85 wt%, NZ) catalysts. For the promoted samples, aqueous solutions of potassium carbonate (Acros, >99%), lanthanum nitrate hexahydrate (Alfa Aesar, >99.9%) and iron (III) nitrate nonahydrate (Sigma Aldrich, ≥ 98%) were co-impregnated with the Ni precursor aqueous solution on the ZrO_2 support to synthesise the Ni-La/ZrO_2 (15/5/85 wt%, NLZ), Ni-Fe/ZrO_2 (15/5/85 wt%, NFZ) catalysts. After impregnation, the resulting mixture was dried overnight at 80 °C and then calcined at 500 °C for 5 h, if not stated differently. For Ni-K/ZrO_2 (15/5/80 wt%, NKZ), ZrO_2 was first impregnated with the Ni precursor, dried overnight at 80 °C and then calcined at 500 °C for 5 h. The resulting powder was further impregnated with an aqueous solution of K_2CO_3, dried overnight at 80 °C and then calcined at 500 °C for 5 h.

2.2. Catalyst characterization

Powder X-ray diffractograms were acquired on a Bruker D8 Advance Diffractometer with Bragg-Brentano geometry using monochromatic Cu Kα (λ = 1.5406 Å) or Co Kα radiation (λ = 1.7902 Å). BET surface area of the catalysts was determined from N_2 adsorption isotherms at 77 K using a Micromeritics TriStar II 3020 instrument. H_2 temperature programmed reduction (H_2-TPR) was performed on a TPDRO 1100 (Thermo Fisher Scientific) equipped with a TCD detector. 50 mg of catalyst material was pretreated at 300 °C for 30 min under N_2 flow (30 mL min^{-1}) and the sample was cooled to 30 °C under N_2. Then the gas atmosphere was changed to H_2 (30 mL min^{-1}, 5 vol% in N_2). The sample temperature was raised from 30 to 800 °C at the ramp rate of 10 °C min^{-1} monitoring H_2 consumption. NH_3 temperature programmed desorption was performed in a Micromeritics Autochem II 2920 instrument equipped with TCD detector. Samples were pretreated in He (25 mL min^{-1}) for 1 hr at 600 °C (heating rate 10 °C min^{-1}), then cooled down to 120 °C and saturated with NH_3 flow for 1 hr (25 mL min^{-1}, 1.5 vol% in He). After that, the desorption step took place in He (25 mL min^{-1}) from 120 to 600 °C (heating rate 10 °C min^{-1}). Thermogravimetric analysis (TGA) of the spent samples was carried out in a METTLER TOLEDO SF/1100 thermogravimetric analyser by heating them up to 1000 °C at a rate of 10 °C min^{-1} under synthetic air flow (100 mL min^{-1}). The same TGA equipment was employed for CO_2-TPD studies. Catalyst powder were loaded in the TGA analyser and pretreated in N_2 (100 mL min^{-1}) at 450 °C (heating rate 10 °C min^{-1}). After that, a pure CO_2 flow was passed at room temperature (100 mL min^{-1} 1 h). The atmosphere was then switched to N_2 and catalysts were heated up to 450 °C (heating rate 10 °C min^{-1}) measuring the weight change associated to CO_2 desorption. Transmission electron microscopy (TEM) of fresh and spent samples (after DC-DRM at 800 °C) was carried out on a Jeol JEM1400 plus TEM instrument.

2.3. Catalytic testing

The configuration of the catalytic reactor setup was similar to the one described in previous works.[36,37] The gas controlling part consisted of mass flow controllers (MFCs, Bronkhorst) and two electric 4-way valves to switch among different gas flows at the inlets. The catalyst powder was pelletised, crushed and sieved in 200–300 μm range. A tubular quartz tube reactor (0.4 mm ID, 0.6 mm OD) was filled with 200 mg of catalyst. Before reaction, the catalyst underwent a reducing pretreatement under 50 mL min^{-1} of pure H_2 at 500 °C for 1 h, unless stated differently. The temperature of the bed was controlled by a thermocouple inserted in the quartz reactor. Catalytic performance was evaluated under DC-DRM conditions at different temperatures (450 °C, 550 °C, 650 °C, 750 °C and 800 °C) and ambient pressure. The composition of the reactor effluent gas mixture was quantified by FT-IR spectroscopy (ALPHA, Bruker, 5 s per spectrum). Valve switching and spectral acquisition were synchronised by LabView software. Each cycle of operation consisted of the alternation of 4 different phases (XFYF, where X = 10.6 vol% CO_2 in He, F = 100 vol% He flush, Y = 11.2 vol% CH_4 in N_2, F = 100 vol% He flush, total flowrate 50 mL min^{-1}, unless stated differently), starting with the oxidising CO_2 stream. In each experiment, the synchronised FTIR spectra acquisition started with the first CO_2 reactant pulse. The data presented were obtained from the average of at least 5 cycles of operation, after a stable and reproducible composition of the effluent was achieved. Conversion of CH_4 and CO_2 pulses were defined as

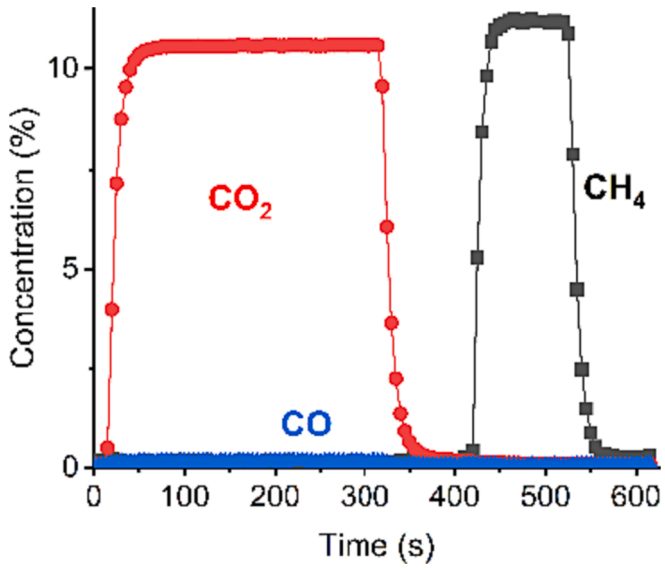

Fig. 1. Reactor outlet gas concentrations obtained by FTIR spectroscopy during a blank DC-DRM experiment (SiC bed). DC-DRM cycle consists of the alternation of diluted CO_2 feed (10.6 vol% in He, 0–300 s), He flush (300–405 s), diluted CH_4 feed (11.2 vol% in N_2, 405–510 s), He flush (510–615 s). Total flow rate was kept at 50 mL min^{-1}. Results are averaged over multiple stable cycles of operation.

$$X = \frac{n_b - n_r}{n_b} \quad (8)$$

where n_b and n_r are the moles of reactant (CO_2 or CH_4) detected during a blank experiment and the reaction, respectively. Mass spectrometry (Omnistar, Pfeiffer Vacuum) was implemented to detect IR-transparent H_2 in the reactor effluent.

2.4. Operando thermal imaging of the catalyst bed

To investigate the spatial development of temperature gradients in the catalytic bed, an infrared thermal camera (IR camera, Micro-SWIRtm 320CSX Camera, Sensors Unlimited) is employed and placed on top of the reactor furnace. A glass-covered window opened at the top of the reactor furnace allow retrieving the IR radiation emitted by the hot catalytic bed and record its longitudinal temperature profile.

3. Results & discussion

Unsteady-state operation for dry reforming of methane was achieved experimentally by exposing the catalytic bed to the pulsed alternation of a CH_4-containing and a CO_2-containing feed for several cycles of operation. The gas composition of the reactor outlet stream was analysed by infrared spectroscopy. Fig. 1 reports the gas concentration profiles obtained for a blank experiment, employing a SiC bed. In a typical DC-DRM cycle, a CO_2 pulse (0–300 s) was initially sent to the reactor, followed by the reducing CH_4 pulse (405–510 s). For the purposes of this investigation, inert flushing phases (He, 300–405 s and 510–615 s) were introduced between the CO_2 and CH_4 pulses to avoid mixing of the reactants phases, to eliminate side reactions activated in co-feed conditions and thus isolate the role of the different catalytic materials.

3.1. Screening of irreducible metal oxide supports

First, SiO_2, ZrO_2 and γ-Al_2O_3 were screened as support materials for the catalytic system. The Ni precursor was added to the support via incipient wetness impregnation in order to obtain a final composition of 15 wt% Ni on the metal oxide support. X-ray diffractograms of the synthesised samples are reported in supplementary information (Fig. S1). Considering the unsteady-state nature of the DC-DRM operation, an optimal catalyst should provide high activity in CH_4 decomposition and gasification of the carbon deposits by CO_2 with high efficiency. In this regard, the ratio between the converted CO_2 and the converted CH_4 (X_{CO2}/X_{CH4}) represents a useful descriptor to evaluate the catalytic performance. Considering the stoichiometry of the DC-DRM reaction, a catalyst with X_{CO2}/X_{CH4} ratio approaching 1 can provide high stability of the catalytic process by avoiding the accumulation of carbon deposits and at the same time guaranteeing the stoichiometric H_2/CO ratio of 1 in the product stream.

The screening of the support materials was conducted at mild reaction temperatures (550 and 650 °C), in order to highlight the contribution of the support to the reaction. At higher temperatures, extensive carbon deposition takes place and the peculiar role of the support in the reaction is less evident. Fig. 2 reports the conversions of the CO_2 (X_{CO2}) and CH_4 (X_{CH4}) pulses (as defined in Eq. (8)) and their ratio X_{CO2}/X_{CH4} for the different Ni-supported catalysts.

ZrO_2- and γ-Al_2O_3-supported catalysts displayed similar catalytic activity and, compared to the SiO_2-supported catalyst, they exhibited higher CO_2 conversion at both temperatures investigated and higher CH_4 conversion at 650 °C. The results clearly indicate a role played by the metal oxide support in the catalytic conversion of CO_2 and CH_4. Uncoordinated surface sites in metal oxides can exhibit acidic or basic character which directly influences the interaction with gaseous reactants. This is particularly of interest in the case of DRM catalysis. It is commonly recognised that SiO_2 support does not display prominent acidic or basic properties while ZrO_2 and Al_2O_3 can act as acid-base bifunctional catalyst.[38–40] NH_3-TPD and CO_2-TPD tests

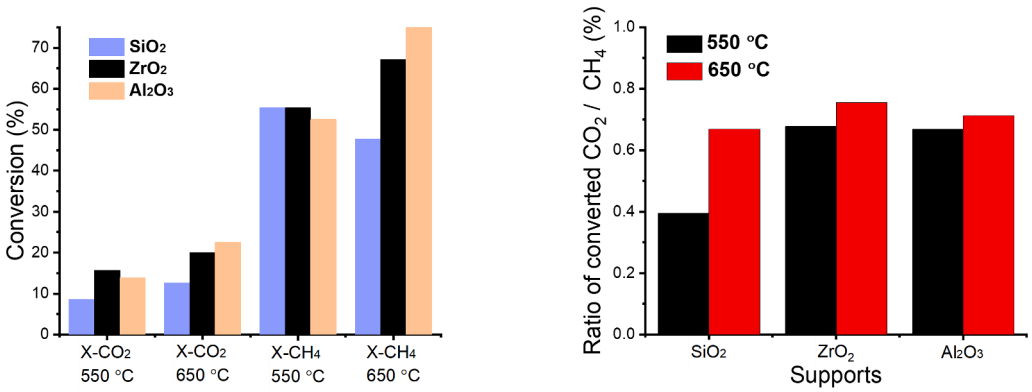

Fig. 2. CO_2 and CH_4 conversion (X_{CO2}, X_{CH4}) obtained during DC-DRM at 550 °C and 650 °C on different metal oxide-supported Ni catalysts (left, 15 wt% Ni) and ratio of converted CO_2/CH_4 (right). DC-DRM cycle consists of the alternation of diluted CO_2 feed (10.6 vol% in He, 0–300 s), He flush (300–405 s), diluted CH_4 feed (11.2 vol% in N_2, 405–510 s), He flush (510–615 s). Total flow rate was kept at 50 mL min^{-1}. Results are averaged over multiple stable cycles of operation.

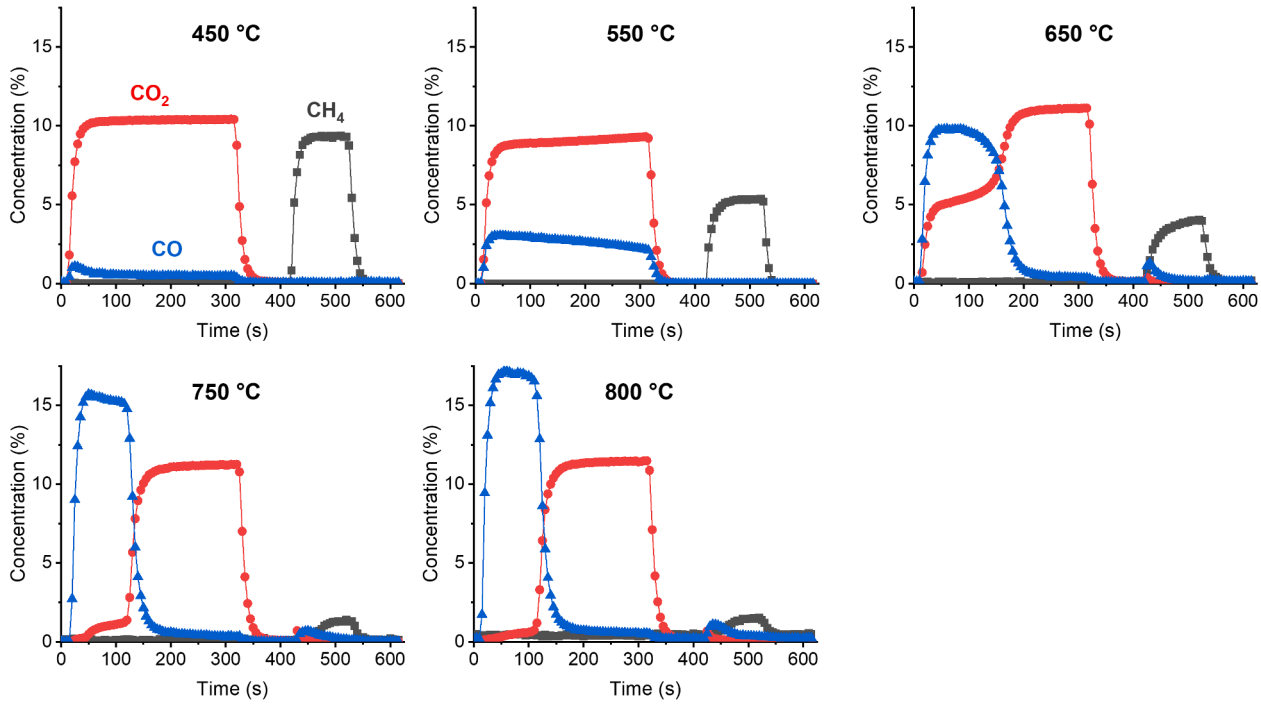

Fig. 3. Reactor outlet gas concentrations obtained by FTIR spectroscopy during DC-DRM experiments on Ni-ZrO_2 catalyst (15 wt% Ni, NZ) at different temperatures. DC-DRM cycle consists of the alternation of diluted CO_2 feed (10.6 vol% in He, 0–300 s), He flush (300–405 s), diluted CH_4 feed (11.2% in N_2, 405–510 s), He flush (510–615 s). Total flow rate was kept at 50 mL min^{-1}. Results are averaged over multiple stable cycles of operation.

(Supplementary Information, Figs. S2–S4) confirmed these acidic and basic properties for the metal oxide-supported Ni catalysts synthesised in this work. The adsorption of CO_2 molecule, a Lewis acid, can be favoured in presence of surface basic sites, while acid sites promotes the cracking of methane.[41,42] Decreasing the acidity of the Ni/Al_2O_3 catalyst by addition of P, Bang et al.[43] observed a decrease in the initial CH_4 and CO_2 conversion. At the same time, the catalyst with lowest acidity showed limited deactivation by carbon deposition and more stable performances, indicating that C gasification by CO_2 is enhanced by the increased basicity introduced by P.

Specifically for DC-DRM operation, the ability to provide both basic and acidic functionalities at the surface can orient the choice of the support material, in order to approach a ratio of converted CH_4 and CO_2 (X_{CO2}/X_{CH4}) close to 1, an important condition for the stability of the performances. Our results indicated that, thanks to the good performance in CH_4 and CO_2 conversions and the X_{CO2}/X_{CH4} ratio approaching 1, ZrO_2 demonstrates promising potential as support for DC-DRM catalysts and thus it was chosen for the following investigations.

3.2. Reaction temperature

Fig. 3 shows the reactor outlet stream composition during DC-DRM catalytic tests performed at different temperatures on the Ni/ZrO_2 catalyst. The results presented were obtained by averaging six cycles of stable operation. During the CH_4 pulse, solid carbon is deposited onto the catalyst, and in the subsequent CO_2 pulse, it serves as intermediate for the formation of CO via gasification reaction. For consistency, the concentration profiles during the CO_2 pulse is shown first in the Figures. In Ni-based catalysts, carbon nanofibers grow on the catalytic material as a result of the CH_4 decomposition. Importantly, the rate of gasification of carbon nanofibers by CO_2 is substantially higher compared to graphite or other carbon materials (carbon black, activated carbon).[44] When the temperature is sufficiently high, the CO_2 pulse could induce the carbon oxidation, thus complete regeneration of the activity towards CH_4 decomposition at each cycle, enabling the continuous DC-DRM operation.

In agreement with the endothermic nature of the decomposition reaction (Eq. (2)), the conversion of CH_4 is expected to increase with temperature. At the switch to the CH_4 pulse (405–510 s), the detection of CH_4 was immediate at temperatures between 450 and 650 °C. However, at 750 °C and 800 °C, the signal of CH_4 was detected with a delay. The absence of CH_4 signal above the detection limit of the analytic technique (ca. 100 ppm) indicates that very high conversion of the reactant feed was achieved at the beginning of the pulse. Such behaviour reflects the kinetic enhancement of CH_4 conversion at high temperatures and, accordingly, an increase in the rate of coking.

Above 650 °C, little CO and CO_2 formation was detected in the CH_4 pulse (405–510 s), revealing the ability of the catalyst to provide oxidising species. Considering the negligible reducibility of the ZrO_2 support, oxidation of CH_4 to CO and CO_2 may be caused by the presence of NiO species, formed upon exposure to the CO_2 pulse. The coke gasification to CO takes place in the CO_2 pulse (0–300 s). At 450 and 550 °C, the coke gasification is limited, thus explaining the low CO_2 conversion profile observed. The concentration of CO in the product stream reached a maximum and then slowly decayed during the CO_2 pulse. However, at 650 °C, the formation of CO becomes favourable and most of the coke was removed in the first 120 s of the CO_2 pulse. At even higher temperatures, the kinetic of coke gasification is greatly enhanced bringing to fast and full conversion of CO_2. At 800 °C, the ZrO_2-supported catalyst was able to continuously provide high conversion of CO_2 and CH_4 in DC-DRM operation.

3.3. Promoters for DC-DRM catalysts

Fast deactivation of the catalyst in conventional DRM is commonly addressed to accumulation and uncontrolled growth of carbon deposits. Functionalisation of the catalyst material by addition of metal promoters is then a strategy to reduce the extent of coking and enhance the catalyst stability.[45] In the perspective of DC-DRM operation, fast coking is desirable when associated to the fast and complete conversion of the CH_4 pulse, as long as complete conversion of C deposits and regeneration of the activity is ensured in the CO_2 pulse. In this sense, an ideal

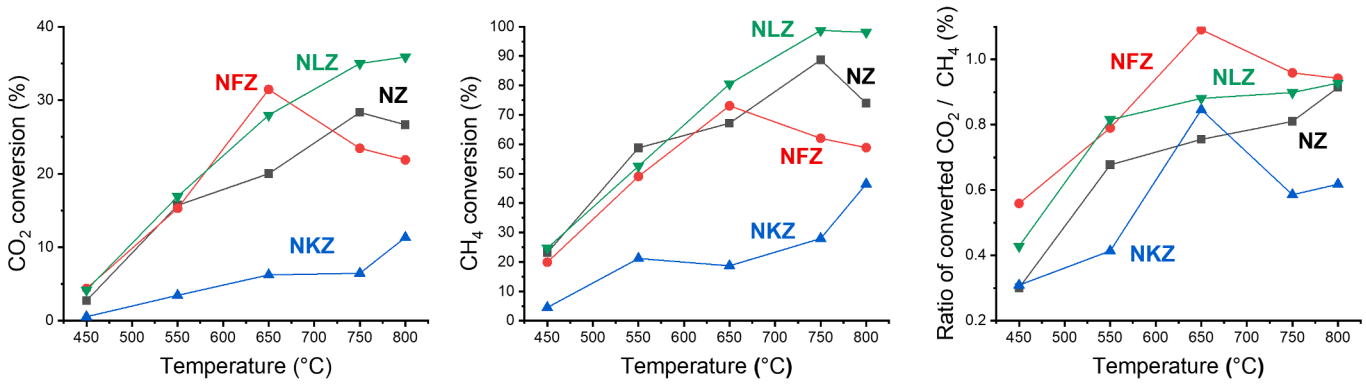

Fig. 4. Comparison of CO_2 conversion (left), CH_4 conversion (middle) and ratio of converted CO_2/CH_4 (right) during DC-DRM performed at different temperatures over unpromoted Ni/ZrO_2 (15 wt% Ni) and promoted Ni/ZrO_2 catalysts ('NXZ' where 'X' is 'F' for Fe, 'L' for La and 'K' for K; 15 wt% Ni, 5 wt% X). DC-DRM cycle consists of the alternation of diluted CO_2 feed (10.6 vol% in He, 0–300 s), He flush (300–405 s), diluted CH_4 feed (11.2% in N_2, 405–510 s), He flush (510–615 s). Total flow rate was kept at 50 mL min^{-1}. Results are averaged over multiple stable cycles of operation.

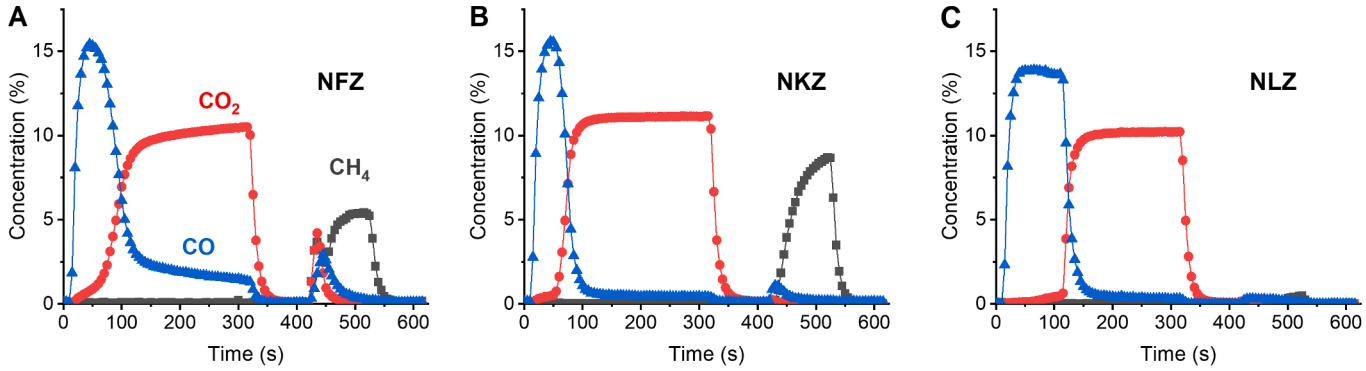

Fig. 5. Reactor outlet gas concentrations obtained by FTIR spectroscopy during DC-DRM experiments at 800 °C on promoted Ni-ZrO_2 catalyst ('NXZ' where 'X' is 'F' for Fe, 'L' for La and 'K' for K; 15 wt% Ni, 5 wt% X). DC-DRM cycle consists of the alternation of diluted CO_2 feed (10.6 vol% in He, 0–300 s), He flush (300–405 s), diluted CH_4 feed (11.2 vol% in N_2, 405–510 s), He flush (510–615 s). Total flow rate was kept at 50 mL min^{-1}. Results are averaged over multiple stable cycles of operation.

catalyst should maximise the conversion of both CO_2 and CH_4 pulses, condition that also reduces the high costs of processing and separation of the product streams (i.e. CO and H_2). As a consequence, it is convenient to investigate the role of metal promoters in the catalytic system in terms of CO_2 and CH_4 conversions and their ratio. Promoted ZrO_2-supported Ni catalysts were prepared by addition of Fe, K or La metal promoters (15 wt% Ni, 5 wt% Fe, K or La). Fig. 4 compares the DC-DRM performance obtained on the unpromoted and promoted catalysts at different temperatures.

It is known that K addition increases the basicity of the catalyst, which favours chemisorption of CO_2 and enhances the gasification of carbon deposits.[46] Looking at Fig. 4, the addition of K (NKZ) drastically reduced the DC-DRM catalytic activity in terms of both CO_2 and CH_4 conversion compared to the unpromoted Ni/ZrO_2 catalyst (NZ) at all temperatures investigated. At 800 °C, only 11% of the CO_2 and 46% of the CH_4 pulses were converted in the K-promoted system. The concentration profiles obtained at 800 °C (Fig. 5) revealed the presence of unreacted CO_2 and CH_4 in the corresponding pulses. In conventional DRM, it has been reported that K improves the catalyst stability by strongly suppressing coke formation.[47] This can be associated to a retarding effect of potassium on the methane decomposition steps (methane dissociation and carbon nucleation).[48] In DC-DRM, this functionality has a negative effect on the global catalytic performance in terms of both CH_4 and CO_2 conversion, with a substantially low X_{CO2}/X_{CH4} ratio. Rather, fast and extensive coking would be desirable as result of the complete CH_4 conversion, and the carbon deposits are expected to be efficiently removed in the CO_2 pulse.

Studies on bimetallic Ni-Fe catalysts reported a positive effect of Fe in DRM catalysis, which improves the gasification of carbon deposits and the resistance to intensive coking.[49] Theofanidis et al.[24] observed that Fe directly participates in the DRM mechanism, mediating the oxidation of C deposits by CO_2. Thanks to its redox properties, Fe gets easily oxidised by the gaseous CO_2 and in turn FeO_x species efficiently oxidise the carbon deposits to form CO and regenerate metallic Fe. H_2-TPR measurements confirmed that, in presence of Fe, the total H_2 consumption increases compared to the unpromoted sample and the reduction peak shifts to lower temperatures (Fig. S5). In terms of catalytic activity towards DC-DRM, the tested Fe-promoted catalyst (NFZ in Fig. 4) showed little improvement in terms of CO_2 and CH_4 conversion compared to the unpromoted Ni/ZrO_2 system. The increased CO_2 conversion at 650 °C can be explained by the oxidation of the iron present in the catalyst. By further increasing the reaction temperature, both CO_2 and CH_4 conversion declined, reaching 22% and 59% at 800 °C, respectively. From the gas concentration profiles obtained at 800 °C (Fig. 5), it is possible to gain further insight about the effect of Fe as promoter. Analysing the CO_2 pulse region (0–300 s), a residual CO_2 signal was detected since the beginning of the cycle associated with a diminished activity in CO_2 conversion. After the initial coke gasification time (ca. 100 s), CO_2 was steadily consumed during the rest of the pulse producing CO. The total higher CO_2 consumption appears then to be linked to the oxidation of the Fe component which proceeded along the whole CO_2 pulse. As a consequence, in the CH_4 pulse, a strong increase in the concentration of the oxidation products (i.e. CO and CO_2) was registered, resulting from the partial and total oxidation of CH_4 by the

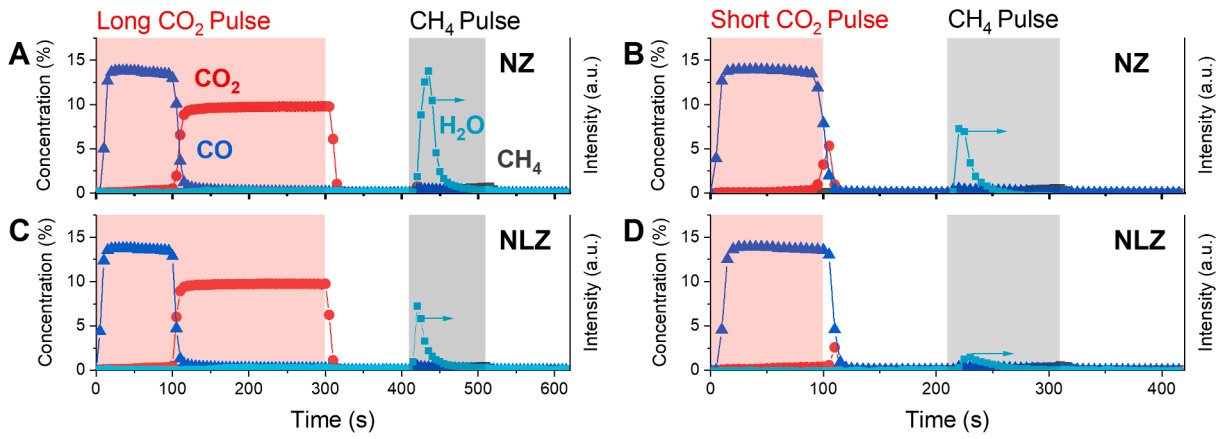

Fig. 6. Reactor outlet gas concentrations obtained by FTIR spectroscopy during DC-DRM experiments at 800 °C on unpromoted Ni-ZrO_2 (A-C; 15 wt% Ni) and Ni-La/ZrO_2 (B-D; 15 wt% Ni, 5 wt% La) catalysts with corresponding FTIR signal of water. Long CO_2 pulse experiments (A-C) consists of the alternation of diluted CO_2 feed (9.9 vol% in He, 0–300 s), He flush (300–405 s), diluted CH_4 feed (10.5 vol% in N_2, 405–510 s), He flush (510–615 s). Short CO_2 pulse experiments (C-D) consists of the alternation of diluted CO_2 feed (9.9 vol% in He, 0–100 s), He flush (100–210 s), diluted CH_4 feed (10.5 vol% in N_2, 210–310 s), He flush (310–420 s). Total flow rate was kept at 50 mL min^{-1}. Results are averaged over multiple stable cycles of operation. For this experiment, catalyst batches calcined at 800 °C were employed.

catalyst lattice oxygen species.

As evident in Fig. 4, the addition of La (NLZ) improved the CO_2 and CH_4 conversions in the whole temperature range, ensuring the best performance for DC-DRM operation among the studied catalysts. Looking at the profile obtained at 800 °C (Fig. 5) on the NLZ catalyst, periods of almost complete CO_2 and CH_4 conversion are exhibited during the respective pulses. At this temperature and duration of the pulses, 36% of total CO_2 and 98% of total CH_4 fed to the reactor were converted. The ratio between the amount of CO_2 and CH_4 converted tended to 1, meaning that most of the carbon deposits can be removed in the CO_2 phase, a key condition for the long-term stability of the catalytic activity. La addition promotes Ni-based catalyst performance for DRM in terms of activity and catalyst stability. The formation of a La_2OCO_3 phase in DRM conditions mediates the interaction of the catalyst with CO_2 and enhances the gasification of deposited carbon.[50] Moreover, high dispersion of La demonstrated to protect Ni particles from oxidation and sintering.[51] In terms of protecting the active metallic Ni phase from oxidation, the promoting effect of La is evidenced in Fig. 6. In DC-DRM reaction, the oxidative conditions of the CO_2 pulse promote oxidation of the Ni phase, which represents a well-known cause of catalyst deactivation towards CH_4 decomposition.[44,52] In the case of unpromoted Ni/ZrO_2 catalyst (Fig. 6A), water signal is detected in the reactor outlet stream during the CH_4 pulse. The water formation indicates the presence of an oxygen source in the catalyst, which can be identified in a partially oxidised Ni phase formed upon exposure of metallic Ni to the long CO_2 pulse. In the reducing pulse, the NiO species can be reduced by the H_2 produced or by the CH_4 itself, as indicates the small release of CO_2 at the beginning of the pulse. Keeping Ni in a reduced state is fundamental to maintain high CH_4 decomposition yields. DC-DRM operation intrinsically guarantees a limitation of the extent of Ni oxidation, thanks to the short oxidising pulse. By reducing the CO_2 pulse duration to the carbon gasification period (i.e. time of maximum conversion of CO_2, 0–100 s in Fig. 6A), the extent of Ni oxidation can be partially reduced, as shown in Fig. 6B. Ni oxidation by CO_2 is drastically prevented in the La-promoted catalyst, as shown by the decreased release of water in the CH_4 pulse (Fig. 6C) compared to the unpromoted sample, likely due to a preferential interaction of CO_2 with the basic La-derived phase. By optimising the duration of the CO_2 pulse and limiting it to the carbon gasification period (0–100 s in Fig. 6C), a minimum water release is detected in the CH_4 pulse, indicating the almost full suppression of the Ni oxidation phenomenon in presence of La (Fig. 6D).This allows to obtain almost total conversion of the CO_2 pulse together with the prevention of Ni

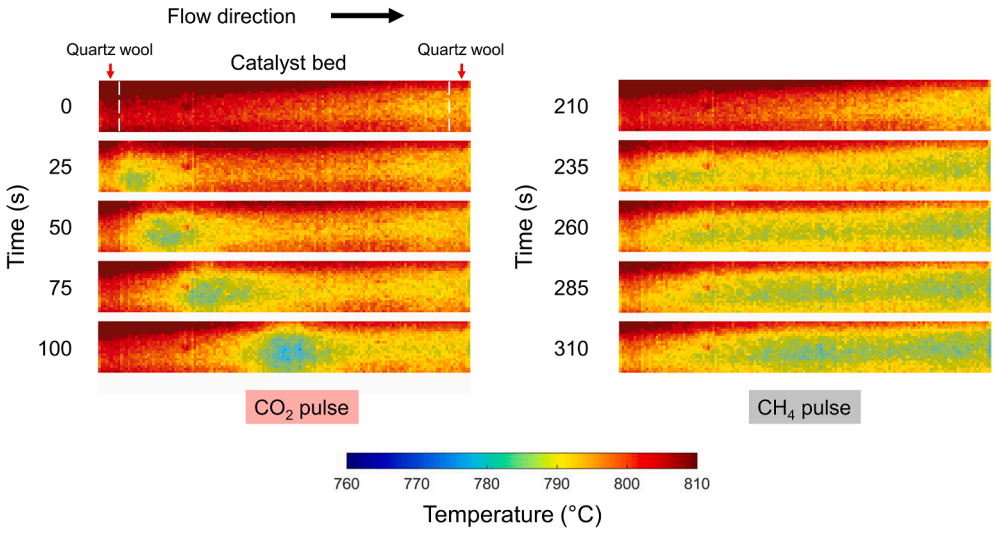

Fig. 7. Operando IR thermal camera imaging of Ni-La/ZrO_2 (15 wt% Ni, 5 wt% La) catalytic bed during DC-DRM operation at 800 °C. Images acquired during diluted CO_2 pulse (0–100 s, left) and diluted CH_4 pulse (210–310 s, right). Reactor outlet gas concentrations are reported in Fig. 6D.

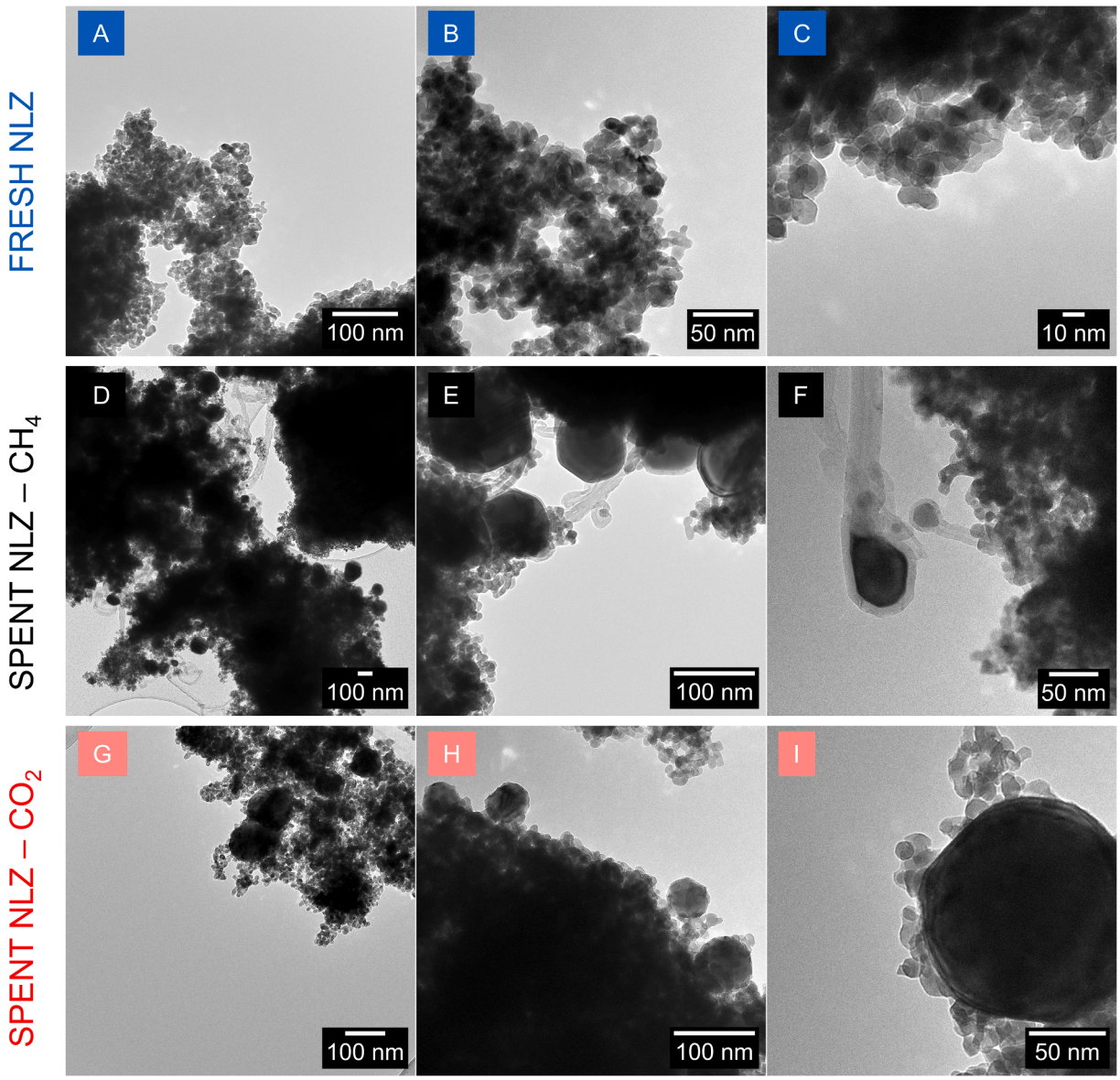

Fig.8. TEM micrographs of the fresh NLZ sample calcined at 500 °C (A-C) and spent NLZ samples after DC-DRM at 800 °C with reactions stopped at the end of the CH_4 pulse (D-F) and at the end of the CO_2 pulse (G-I). DC-DRM cycle consists of the alternation of diluted CO_2 feed (9.9 vol% in He, 0–100 s), He flush (100–210 s), diluted CH_4 feed (10.5 vol% in N_2, 210–310 s), He flush (310–420 s). Total flow rate was kept at 50 mL min^{-1}. After stopping the reaction, the catalysts were brought to room temperature in inert flush (He) at 10 °C min^{-1} cooling rate.

oxidation, thus improving the long-term stability of the catalyst performances.

In such operating conditions, it is possible to perform continuous DC-DRM operation on the NLZ system with about 99% conversion of CH_4 and 96% conversion of CO_2, having CO as main product in the oxidising pulse and H_2 as main product in the reducing pulse. Quantitative evaluation of the H_2 produced was conducted by implementing mass spectrometry during DC-DRM at 800 °C on NLZ (Supplementary Information, Fig. S6). The results confirmed the selective conversion of CH_4 to H_2 and its production in amounts comparable to the stoichiometry of decomposition reaction.

3.4. Operando IR thermal imaging

In DC-DRM, coke acts as intermediate between the H_2 production from CH_4 and the subsequent CO generation from CO_2. The alternation between the two short reactant pulses is expected to increase the stability of the process compared to conventional co-feed operation. Fast coking of the catalyst is targeted in the CH_4 pulse, then the reactant feed is switched to CO_2 to selectively and effectively gasify the coke to CO.

Since both CH_4 decomposition and C gasification by CO_2 are endothermic reactions, monitoring the temperature of the catalyst bed during reaction can provide insights about the coke-mediated mechanism of DC-DRM. Fig. 7 shows the temperature profile of the catalyst bed obtained during the CO_2 and CH_4 pulses of DC-DRM at 800 °C on the NLZ catalyst (catalytic results shown in Fig. 6D).

A clear temperature decrease was observed for both phases. During the CH_4 pulse, the reduction in temperature took place simultaneously from the front to the end of the catalytic bed until the end of the reduction pulse. This indicates that the catalyst is actively converting CH_4, releasing H_2 in the product stream and accumulating C over the surface of the whole catalyst bed. Considering the homogeneous activity of the bed, accumulation of carbon deposits at the front positions may be favoured in fixed bed configuration, resulting in spatial gradients of coke accumulation. High CH_4 conversion was maintained for the entire duration of the pulse, indicating that the reactant feed was switched

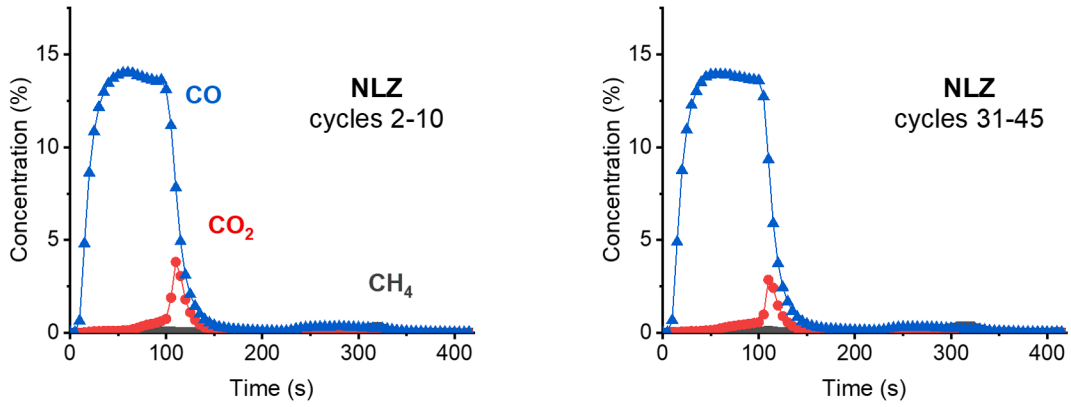

Fig. 9. Reactor outlet gas concentrations obtained by FTIR spectroscopy during DC-DRM stability test at 800 °C on La-promoted Ni/ZrO_2 catalyst (15 wt% Ni, 5 wt% La, NLZ). DC-DRM cycle consists of the alternation of diluted CO_2 feed (9.9 vol% in He, 0–100 s), He flush (100–210 s), diluted CH_4 feed (10.5 vol% in N_2, 210–310 s), He flush (310–420 s). Total flow rate was kept at 50 mL min^{-1}. Results presented are averaged of cycles 2–10 (left) and cycles 31–45 (right) of operation.

before catalyst deactivation.

Interestingly, thermal imaging of the bed during the CO_2 pulse showed a clear 'cold spot' that propagated in the direction of the flow, reflecting the progress of the endothermic gasification reaction along the catalytic bed. The carbon deposits accumulated in the previous CH_4 pulse were gasified to CO resulting in high CO_2 conversions (96%). The cold spot represents a portion of the catalytic bed in which intense gasification of the C takes place, with CO_2 being largely converted. The removal of C species was completed progressively along the catalytic bed, as indicated by the 'cold spot' moving towards the end of the bed. At the end of the CO_2 pulse (100 s), the majority of the carbon deposits were gasified and unreacted CO_2 started to be detected in the reactor effluent stream.

3.5. Transmission electron microscopy (TEM)

The insights into the coke-mediated mechanism obtained by *operando* IR thermal imaging were further confirmed by Transmission Electron Microscopy (TEM). Fig. 8 presents the TEM micrographs obtained for the fresh and spent NLZ catalyst samples. For the fresh NLZ sample calcined at 500 °C (Fig. 8A-C), the absence of big agglomerates indicated a good dispersion of the Ni and La phases on the ZrO_2 support. In Fig. 8C in particular, small particles (1–2 nm) were spotted on top of the ZrO_2 particles (10 nm), suggesting a high dispersion of the active phases obtained with the synthesis. To investigate the formation of coke and the effectiveness of its gasification during DC-DRM at 800 °C, spent samples were collected after stopping the reaction at the end of the CH_4 pulse (Fig. 8D-F) and at the end of the CO_2 pulse (Fig. 8G-I). The high temperatures of reduction pre-treatment and DC-DRM reaction promoted the sintering of the metallic Ni phase, which tended to form agglomerates of size up to 100 nm. As expected, extensive coking of the catalyst took place in the CH_4 pulse, resulting in the pervasive growth of carbon-based structures on the catalyst (Fig. 8D). There is consolidated knowledge about the decomposition of light hydrocarbons on Ni, with formation of two main types of carbon structures, namely carbon whiskers and graphitic layers.[48] Our results indicates that bigger Ni agglomerates (>50 nm) were generally encapsulated in thin graphitic layers, while smaller Ni particles detached from the support and dynamically participated to the growth of carbon whiskers, forming filamentous hollow carbon structures of various diameters and lengths. This finding is in agreement with *in situ* TEM investigations that observed a dynamic reshaping of nickel nanocrystals taking place during the growth of carbon nanofibers on Ni.[53,54] TEM micrographs of the spent sample after the CO_2 pulse (Fig. 8 G-I) shows that the majority of the carbon species were effectively removed to form CO and the catalyst was regenerated. A wide distribution of sizes for Ni phase was found, with sintered particles in the range of 50–80 nm. At reaction conditions, however, sintering did not cause deactivation of the catalyst performances.

3.6. Stability of La-promoted Ni/ZrO_2

The accumulation of solid carbon deposits in catalytic DRM reactors leads to several complication, including catalyst fouling, pressure build-up and reactor blockage.[55] DC-DRM principle of exposing the catalysts to short reducing and oxidising pulses is expected to limit the irreversible accumulation of stable carbon deposits in CH_4, facilitating their complete gasification in CO_2 and regenerating the catalytic activity at each cycle. Fig. 9 shows the results obtained for a NLZ catalyst during extended catalytic activity tests at 800 °C (45 reaction cycles). Comparing the catalytic activity of the initial cycles (2–10) with the last 15 cycles of operation (31–45), a remarkable stability of the performances was observed in terms of CO_2 and CH_4 conversion, with the absence of noticeable deactivation trends. These results indicates the ability of the NLZ system to provide high and stable conversion of CO_2 and CH_4 in DC-DRM conditions. After the last CO_2 pulse of the stability test, the reaction was stopped and the catalyst cooled down in He for ex-situ investigation.

The high reaction temperature and highly reducing conditions of DC-DRM are expected to promote the sintering of Ni particles. The changes observed in X-ray diffractograms before and after the stability tests (Supplementary Information, Fig. S7) indicated the presence of sintering phenomena involving both the Ni crystallites and the supports, as already shown in TEM micrographs of the spent NLZ sample (Fig. 8). This is expected, considering that the reaction was performed at temperature substantially higher than the calcination conditions (500 °C, air). The Ni and support sintering at high temperatures was also evident from the drop of the BET surface area of the spent sample after DC-DRM stability test (Table S1). However, the activity of the catalysts in DC-DRM was not undermined by the observed formation of Ni crystallites, indicating that their growth is controlled on the ZrO_2 support. The exposure of the catalyst to short oxidative/reducing pulses seems to prevent fast and irreversible deactivation of the catalytic system. In fact, a NLZ catalyst synthesised with calcination at 800 °C showed similar catalytic behaviour (Fig. 6B-D), despite the agglomeration of NiO in the fresh sample suggested by the increased degree of crystallinity for the NiO reflexes in XRD (Fig. S7). Interestingly, no drops in the BET surface area after reaction was noticed for the NLZ catalyst calcined at 800 °C (Table S2). These results confirmed that the ZrO_2-supported catalytic system is able to withstand DC-DRM reaction conditions and control the sintering of active metals and support without any noticeable deactivation trend in the first 4.5 h of operation.

Extensive coking is another common cause for catalyst deactivation in DRM. When the NLZ catalyst was tested for conventional DRM

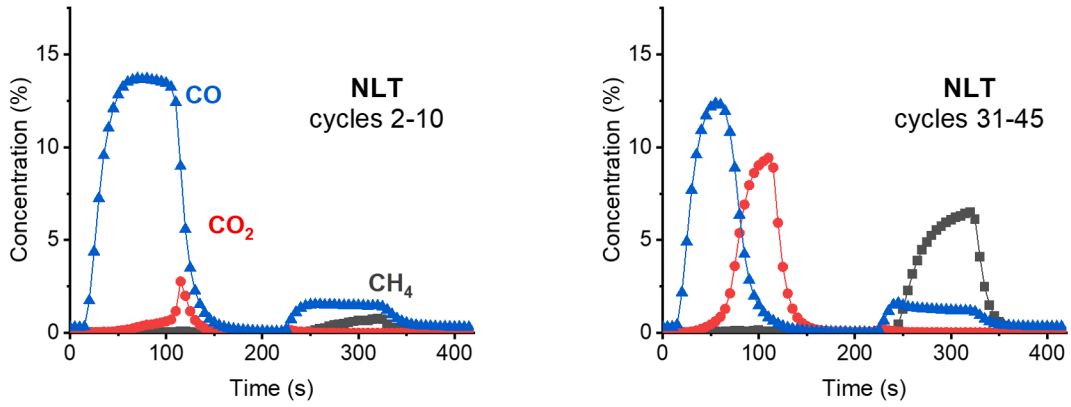

Fig. 10. Reactor outlet gas concentrations obtained by FTIR spectroscopy during DC-DRM stability test at 800 °C on La-promoted Ni/TiO_2 catalyst (15 wt% Ni, 5 wt % La, NLT). DC-DRM cycle consists of the alternation of diluted CO_2 feed (0–100 s), He flush (100–210 s), diluted CH_4 feed (210–310 s), He flush (310–420 s). Total flow rate was kept at 50 mL min^{-1}. Results presented are averaged of cycles 2–10 (left) and cycles 31–35 (right) of operation.

(800 °C, 50 mL min^{-1}, CO_2 10 vol%, CH_4 10 vol%), a fast pressure build-up was registered in the reactor (>0.5 bar), requiring to stop the reaction after 15 min of operation. Compared to the co-feed conditions, the separation of the CO_2 and CH_4 pulses in DC-DRM prevents the accumulation and uncontrolled growth of carbon deposits and allows the complete regeneration of the catalyst at each cycle. Similarly, no increase in pressure drop has been observed during cyclic alternation of CH_4 decomposition and C gasification by steam on Ni-based catalysts. [56] Notwithstanding, analysis of the NLZ catalyst after DC-DRM revealed the presence of a limited amount of carbon deposits after 45 cycles of operation at 800 °C. Thermogravimetric analysis (Supplementary Information, Fig. S8) indicated the presence of solid carbon deposits in the spent NLZ catalyst, which were removed in air below 600 °C. Although the extent of carbon accumulation did not cause deactivation of the catalyst, optimising the catalytic material for complete carbon gasification can be beneficial for long-term operation. Extending the length of the CO_2 pulse can improve the gasification of coke, at the price of purity of the product stream and of the Ni oxidation enhancement. Engineering of several reaction parameters, including the volumetric flow rate and composition of reactant feeds, together with the optimisation of the catalyst composition can target the full removal of carbon deposits in view of long-term utilisation of the catalyst.

3.7. Reducible metal oxide supports for DC-DRM

Compared to irreducible metal oxides, the employment of a reducible metal oxide support offers the possibility of directly oxidising CH_4 in the reducing pulse thanks to the active participation of the lattice oxygen to the reaction. The introduction of an additional oxidant species, represented by the lattice oxygen species of the reducible oxide, is also expected to enhance the selective gasification of carbon deposits, thus limiting their accumulation. Employing TiO_2 rutile as support material, a La-promoted Ni catalyst (15 wt% Ni, 5 wt% La) was prepared by incipient wetness impregnation and tested for DC-DRM. The results of a long-term catalytic test (45 cycles) are shown in Fig. 10.

In the first 10 cycles of operation, the TiO_2-supported system (NLT) exhibited high conversions of CO_2 and CH_4. Noticeably, the behaviour in the reducing CH_4 pulse was significantly different from the one observed in the ZrO_2-supported counterpart. Employing the reducible TiO_2 as support enabled a constant supply of lattice oxygen species for the selective oxidation of CH_4 or carbon deposits to CO. Direct participation of the TiO_2 lattice oxygen in the selective oxidation of CH_4 was already observed in Chapter 4. The high stability of surface oxygen vacancy in rutile TiO_2 is expected to favour the removal of lattice oxygen which can efficiently oxidise the carbon deposits on the catalytic surface.[57].

This contribution of lattice oxygen from the support to form CO directly changes the composition of the product mixture in the CH_4 pulse from pure H_2 to a H_2-rich syngas mixture (Supplementary Information, Fig. S9). By proper tuning of the lattice oxygen diffusion rate, as well as the composition of the reactant stream, a versatile and valuable syngas mixture can be targeted as direct product of the CH_4 pulse, bringing additional benefits to the process including the softening of technological requirements associated with pure H_2 streams (explosion limit, thermal conductivity, pipelines specifications). In the subsequent oxidative pulse, high CO_2 conversion were maintained, confirming the ability of the systems to provide efficient gasification of the carbon deposits together with the replenishment of the lattice vacancies and reoxidation of the metal oxide support.

However, after 45 cycles of operation, the TiO_2-supported catalyst showed a marked deactivation, with extensive loss in both CO_2 and CH_4 conversions (Fig. 10). At the same time, the supply of lattice oxygen during the CH_4 pulse was preserved and the release of CO was not affected by the deactivation of the catalyst. Thermogravimetric analysis (Fig. S8) of the spent catalyst revealed no weight loss trend under heating in air up to 1000 °C, indicating that the catalyst is able to efficiently remove the carbon deposits, also thanks to the contribution of oxygen species from the support lattice. Those findings excluded the contribution of solid carbon accumulation in the deactivation of catalyst observed for the TiO_2-supported catalyst. XRD of the spent catalyst (Fig. S7) revealed that narrow metallic Ni reflexes with strong intensity were found in the spent NLT catalyst, indicating the aggregation of Ni particles into big crystallites. Takenaka et al.[58] reported that at low Ni loadings (2.5 wt%), the Ni/TiO_2 system can provide stability of performances in cycles of CH_4 decomposition and regeneration by CO_2. However, a Ni loading of 10 wt% on TiO_2 led to fast deactivation of the catalyst towards CH_4 decomposition, due to agglomeration of the Ni particles in bigger aggregates. Considering the high loadings employed in this work (15 wt% Ni, 5 wt% La), the low surface area and porosity of the TiO_2-supported catalyst compared to the ZrO_2-supported counterpart (Table E1) clearly favoured the aggregation of the Ni particles and the deterioration of the catalytic activity observed.

The addition of TiO_2 to form binary oxides is known to strongly increase the number of surface acidic sites and their strength.[59] In the case of TiO_2-ZrO_2, both acidity and basicity are enhanced by incorporation of TiO_2.[60] In order to combine the stability of performances provided by an irreducible oxide as support (ZrO_2) with the possibility of tuning the product composition and introducing an additional route for coke gasification by a reducible support (TiO_2), a mixed oxide was synthetised targeting a surface doping of ZrO_2 with TiO_2.

For this purpose, ZrO_2 was impregnated with a Ti isopropoxide solution under inert atmosphere to ensure the dispersion of the Ti precursor in the pores of the ZrO_2 template. After this, the catalyst was dried at 80 °C and calcined at 800 °C in air to ensure the formation of the mixed oxide. XRD of the TiO_2-ZrO_2 support (Supplementary

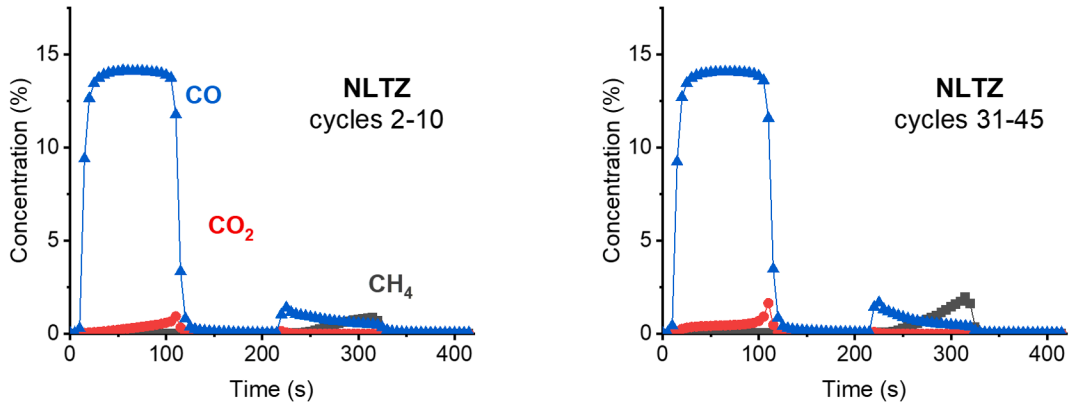

Fig. 11. Reactor outlet gas concentrations obtained by FTIR spectroscopy during DC-DRM stability test at 800 °C on La-promoted Ni/TiO_2-ZrO_2 catalyst (15 wt% Ni, 5 wt% La, NLTZ). DC-DRM cycle consists of the alternation of diluted CO_2 feed (0–100 s), He flush (100–210 s), diluted CH_4 feed (210–310 s), He flush (310–420 s). Total flow rate was kept at 50 mL min^{-1}. Results presented are averaged of cycles 2–10 (left) and cycles 31–35 (right) of operation.

Information, Fig. S10, TZ) showed only reflexes associated to the ZrO_2 phase, suggesting the high dispersion of the Ti-derived phase.

A La-promoted Ni catalyst (NLTZ, Ni 15 wt%, La 5%) was then prepared by incipient wetness impregnation of the TiO_2-ZrO_2 mixed oxide support. NH_3-TPD studies on the NLZ and NLTZ samples indicated that the addition of TiO_2 in the support slightly increased the acidity of the catalyst (Fig. S11, Table S3). Fig. 11 shows the results obtained for CL-DRM at 800 °C on the NLTZ catalyst. Compared to the TiO_2-supported catalyst, the NLTZ system exhibited higher stability of the performances, with high CO_2 conversion maintained after 45 cycles and limited deactivation in terms of CH_4 conversion. Compared to the ZrO_2-supported catalyst, an additional oxidative route was activated by the insertion of TiO_2, which was able to provide lattice oxygen species and led to the formation of CO in the CH_4 pulse. The distinct catalytic functionalities introduced by ZrO_2 and TiO_2 materials were still recognised in the last 15 cycles of DC-DRM operation, although the slight increase of CH_4 signal detected at the outlet in the last 15 cycles suggests a possible weakening in the synergetic behaviour of the two oxidic phase.

Functionalising the ZrO_2 support with a reducible oxide as TiO_2 can enhance the oxidation of the carbon deposits, while maintaining high stability of the catalytic performances and potentially leads the production of a H_2-rich syngas directly in the CH_4 pulse (Fig. S12).

4. Conclusions

With the aim of overcoming the limitations of the conventional co-feed operation, we propose in this work an alternative unsteady-state process named dynamic coke-mediated dry reforming of methane (DC-DRM). In DC-DRM, CO_2 and CH_4 reactant pulses are alternatively sent to the catalytic bed, targeting their complete conversion and achieving the complete separation of the H_2 and CO product stream. Separation of the H_2 and CO_2 streams also suppresses the undesired reverse water–gas shift reaction, which consumes valuable H_2 product in co-feed operation to produce steam. Exposure of the catalyst to short oxidising and reducing pulses can enhance the stability of the system, preventing accumulation of carbon deposits which brings to deactivation and catalyst fouling.

Ni-based catalyst for DC-DRM were synthesised and investigated. Among the irreducible metal oxides tested as support material, ZrO_2 acted as a stable template to the active metal component by containing sintering and ensuring high and comparable CO_2 and CH_4 conversion. On the Ni/ZrO_2 catalytic system, the effect of different metal promoters (La, Fe, K) on the conversion of CH_4 and CO_2 was also evaluated. The addition of Fe resulted in increased oxidation of the catalyst in CO_2 and resulted in total oxidation of CH_4 to undesired CO_2. The presence of K, and the increased basicity of the catalysts, provoked substantial loss in both CH_4 and CO_2 conversions. Distinctively, an enhancement of the DC-DRM performance was found for the La-promoted Ni/ZrO_2 system (NLZ), which enhanced the conversion of CO_2 and suppressed the oxidation of the Ni component. *Operando* IR thermal imaging of the catalytic bed gave relevant insights into the endothermic reaction routes involved in DC-DRM. Fast coking takes place homogenously along the bed during the decomposition of CH_4, while during the CO_2 pulse, a 'cold spot' representing the endothermic gasification of C progressively moves along the flow direction until complete removal of the carbon deposits. The Ni-La/ZrO_2 catalyst provided stable activity and approached complete conversion of the CH_4 and CO_2 reactant pulses to H_2 and CO, respectively, in 45 cycles of operation at 800 °C.

Declaration of Competing Interest

The authors declare the following financial interests/personal relationships which may be considered as potential competing interests: Atsushi Urakawa reports financial support was provided by Japan Science and Technology Agency. Atsushi Urakawa reports a relationship with Japan Science and Technology Agency that includes: funding grants.

Data availability

Data will be made available on request.

Acknowledgements

We thanks the financial support from the Japanese Science and Technology Agency (JST) PRESTO (Grant No. JPMJPR16S3).

Appendix A. Supplementary data

Supplementary data to this article can be found online at https://doi.org/10.1016/j.cej.2023.145641.

References

[1] M.C.J. Bradford, M.A. Vannice, CO_2 reforming of CH_4, Catal. Rev. 41 (1999) 1–42.
[2] J.R. Rostrup-Nielsen, J.H.B. Hansen, L.M. Aparicio, Reforming of hydrocarbons into synthesis gas on supported metal catalysts, J. Jpn. Pet. Inst. 40 (1997) 366–377.
[3] A. Sternberg, A. Bardow, Life cycle assessment of power-to-gas: syngas vs methane, ACS Sustain. Chem. Eng. 4 (8) (2016) 4156–4165.
[4] J.M. Lavoie, Review on dry reforming of methane, a potentially more environmentally-friendly approach to the increasing natural gas exploitation, Front. Chem. 2 (2014) 81.
[5] A.M. Gadalla, B. Bower, The role of catalyst support on the activity of nickel for reforming methane with CO_2, Chem. Eng. Sci. 43 (1988) 3049–3062.

[6] C. Peinado, D. Liuzzi, M. Retuerto, J. Boon, M.A. Peña, S. Rojas, Study of catalyst bed composition for the direct synthesis of dimethyl ether from CO_2-rich syngas, Chem. Eng. J. Adv. 4 (2020), 100039.

[7] G. Celik, A. Arinan, A. Bayat, H.O. Ozbelge, T. Dogu, D. Varisli, Performance of silicotungstic acid incorporated mesoporous catalyst in direct synthesis of dimethyl ether from syngas in the presence and absence of CO_2, Top. Catal. 56 (2013) 1764–1774.

[8] K. Wittich, M. Krämer, N. Bottke, S.A. Schunk, Catalytic dry reforming of methane: insights from model systems, ChemCatChem 12 (2020) 2130–2147.

[9] R. Mann, Catalyst deactivation by coke deposition: Approaches based on interactions of coke laydown with pore structure, Catal. Today 37 (1997) 331–349.

[10] N. Abdel Karim Aramouni, J. Zeaiter, W. Kwapinski, M.N. Ahmad, Thermodynamic analysis of methane dry reforming: Effect of the catalyst particle size on carbon formation, Energ. Conver. Manage. 150 (2017) 614–622.

[11] D. Pakhare, J. Spivey, A review of dry (CO_2) reforming of methane over noble metal catalysts, Chem. Soc. Rev. 43 (2014) 7813–7837.

[12] M. Mohamedali, A. Henni, H. Ibrahim, Recent advances in supported metal catalysts for syngas production from methane, ChemEngineering 2 (2018) 9.

[13] B. Yang, J. Deng, H. Li, T. Yan, J. Zhang, D. Zhang, Coking-resistant dry reforming of methane over Ni/γ-Al_2O_3 catalysts by rationally steering metal-support interaction, iScience 24 (2021), 102747.

[14] N.D. Charisiou, S.L. Douvartzides, G.I. Siakavelas, L. Tzounis, V. Sebastian, V. Stolojan, S.J. Hinder, M.A. Baker, K. Polychronopoulou, M.A. Goula, The relationship between reaction temperature and carbon deposition on nickel catalysts based on Al_2O_3, ZrO_2 or SiO_2 supports during the biogas dry reforming reaction, Catalysts 9 (2019) 676.

[15] J.H. Bitter, K. Seshan, J.A. Lercher, Deactivation and Coke Accumulation during CO_2/CH_4 Reforming over Pt Catalysts, J. Catal. 183 (1999) 336–343.

[16] K. Nagaoka, K. Seshan, K.-I. Aika, J.A. Lercher, Carbon deposition during carbon dioxide reforming of methane – comparison between Pt/Al_2O_3 and Pt/ZrO_2, J. Catal. 197 (2001) 34–42.

[17] J.R. Rostrup-Nielsen, Production of synthesis gas, Catal. Today 18 (1993) 305–324.

[18] M.C.J. Bradford, M.A. Vannice, Catalytic reforming of methane with carbon dioxide over nickel catalysts I. Catalyst characterization and activity, Appl. Catal. A 142 (1996) 73–96.

[19] J.R. Rostrup-Nielsen, Catalytic steam reforming, in: J.R. Anderson, M. Boudart (Eds.), Catalysis: Science and Technology, Vol. 5, Springer, Berlin Heidelberg, Berlin, Heidelberg, 1984, pp. 1–117.

[20] L. Azancot, L.F. Bobadilla, M.A. Centeno, J.A. Odriozola, Effect of potassium loading on basic properties of Ni/$MgAl_2O_4$ catalyst for CO_2 reforming of methane, J. CO2 Util. 52 (2021), 101681.

[21] W. Mo, F. Ma, Y. Ma, X. Fan, The optimization of Ni–Al_2O_3 catalyst with the addition of La_2O_3 for CO_2–CH_4 reforming to produce syngas, Int. J. Hydrogen Energy 44 (2019) 24510–24524.

[22] W.-J. Jang, J.-O. Shim, H.-M. Kim, S.-Y. Yoo, H.-S. Roh, A review on dry reforming of methane in aspect of catalytic properties, Catal. Today 324 (2019) 15–26.

[23] Z. Bian, S. Das, M.H. Wai, P. Hongmanorom, S. Kawi, A review on bimetallic nickel-based catalysts for CO_2 reforming of methane, ChemPhysChem 18 (2017) 3117–3134.

[24] S.A. Theofanidis, V.V. Galvita, H. Poelman, G.B. Marin, Enhanced carbon-resistant dry reforming Fe-Ni catalyst: role of Fe, ACS Catal. 5 (5) (2015) 3028–3039.

[25] J. Zhang, H. Wang, A.K. Dalai, Development of stable bimetallic catalysts for carbon dioxide reforming of methane, J. Catal. 249 (2007) 300–310.

[26] X. Zhu, Q. Imtiaz, F. Donat, C.R. Müller, F. Li, Chemical looping beyond combustion – a perspective, Energ. Environ. Sci. 13 (2020) 772–804.

[27] M. Tang, L. Xu, M. Fan, Progress in oxygen carrier development of methane-based chemical-looping reforming: A review, Appl. Energy 151 (2015) 143–156.

[28] A. Lyngfelt, B. Leckner, T. Mattisson, A fluidized-bed combustion process with inherent CO_2 separation; application of chemical-looping combustion, Chem. Eng. Sci. 56 (2001) 3101–3113.

[29] J. Adanez, A. Abad, F. Garcia-Labiano, P. Gayan, L.F. de Diego, Progress in chemical-looping combustion and reforming technologies, Prog. Energy Combust. Sci. 38 (2012) 215–282.

[30] M. Najera, R. Solunke, T. Gardner, G. Veser, Carbon capture and utilization via chemical looping dry reforming, Chem. Eng. Res. Des. 89 (2011) 1533–1543.

[31] S. Bhavsar, M. Najera, G. Veser, Chemical looping dry reforming as novel, intensified process for CO_2 activation, Chem. Eng. Technol. 35 (2012) 1281–1290.

[32] A. Löfberg, T. Kane, J. Guerrero-Caballero, L. Jalowiecki-Duhamel, Chemical looping dry reforming of methane: toward shale-gas and biogas valorization, Chem. Eng. Process. 122 (2017) 523–529.

[33] S.M. Kim, P.M. Abdala, M. Broda, D. Hosseini, C. Copéret, C. Müller, Integrated CO_2 capture and conversion as an efficient process for fuels from greenhouse gases, ACS Catal. 8 (4) (2018) 2815–2823.

[34] L.C. Buelens, V.V. Galvita, H. Poelman, C. Detavernier, G.B. Marin, Super-dry reforming of methane intensifies CO_2 utilization via Le Chatelier's principle, Science 354 (6311) (2016) 449–452.

[35] V.V. Galvita, H. Poelman, C. Detavernier, G.B. Marin, Catalyst-assisted chemical looping for CO2 conversion to CO, Appl Catal B 164 (2015) 184–191.

[36] L. Hu, A. Urakawa, Continuous CO_2 capture and reduction in one process: CO_2 methanation over unpromoted and promoted Ni/ZrO_2, J. CO2 Util. 25 (2018) 323–329.

[37] D. Pinto, V. van der Bom Estadella, A. Urakawa, Mechanistic insights into the CO_2 capture and reduction on K-promoted Cu/Al_2O_3 by spatiotemporal operando methodologies, Cat. Sci. Technol. 12 (2022) 5349–5359.

[38] K. Tanabe, Solid Acids and Bases: Their Catalytic Properties, Elsevier, 2012.

[39] K. Tanabe, Surface and catalytic properties of ZrO_2, Mater. Chem. Phys. 13 (1985) 347–364.

[40] H.J.M. Bosman, E.C. Kruissink, J. Vanderspoel, F. Vandenbrink, Characterization of the acid strength of SiO2-ZrO2 mixed oxides, J. Catal. 148 (1994) 660–672.

[41] Y. Osamu, N. Takao, O. Kohji, F. Kaoru, Reduction of carbon dioxide by methane with Ni-on-MgO-CaO containing catalysts, Chem. Lett. 21 (1992) 1953–1954.

[42] J.H. Bitter, K. Seshan, J.A. Lercher, The state of zirconia supported platinum catalysts for CO2/CH4 reforming, J. Catal. 171 (1997) 279–286.

[43] S. Bang, E. Hong, S.W. Baek, C.-H. Shin, Effect of acidity on Ni catalysts supported on P-modified Al_2O_3 for dry reforming of methane, Catal. Today 303 (2018) 100–105.

[44] S. Takenaka, E. Kato, Y. Tomikubo, K. Otsuka, Structural change of Ni species during the methane decomposition and the subsequent gasification of deposited carbon with CO_2 over supported Ni catalysts, J. Catal. 219 (2003) 176–185.

[45] R. Franz, D. Pinto, E.A. Uslamin, A. Urakawa, E.A. Pidko, Impact of promoter addition on the regeneration of Ni/Al_2O_3 dry reforming catalysts, ChemCatChem 13 (2021) 5034–5046.

[46] R. Roncancio, J.P. Gore, CO_2 char gasification: A systematic review from 2014 to 2020, Energy Convers. Manage.: X 10 (2021), 100060.

[47] J. Juan-Juan, M.C. Román-Martínez, M.J. Illán-Gómez, Effect of potassium content in the activity of K-promoted Ni/Al_2O_3 catalysts for the dry reforming of methane, Appl. Catal. A 301 (2006) 9–15.

[48] S. Helveg, J. Sehested, J.R. Rostrup-Nielsen, Whisker carbon in perspective, Catal. Today 178 (2011) 42–46.

[49] I.V. Yentekakis, P. Panagiotopoulou, G. Artemakis, A review of recent efforts to promote dry reforming of methane (DRM) to syngas production via bimetallic catalyst formulations, Appl. Catal. B 296 (2021), 120210.

[50] R. Yang, C. Xing, C. Lv, L. Shi, N. Tsubaki, Promotional effect of La_2O_3 and CeO_2 on Ni/γ-Al_2O_3 catalysts for CO_2 reforming of CH_4, Appl. Catal. A 385 (2010) 92–100.

[51] H.-S. Roh, K.-W. Jun, Carbon dioxide reforming of methane over Ni catalysts supported on Al_2O_3 modified with La_2O_3, MgO, and CaO, Catal. Surv Asia 12 (4) (2008) 239–252.

[52] M. Steib, Y.u. Lou, A. Jentys, J.A. Lercher, Enhanced activity in methane dry reforming by carbon dioxide induced metal-oxide interface restructuring of nickel/zirconia, ChemCatChem 9 (20) (2017) 3809–3813.

[53] S. Helveg, C. López-Cartes, J. Sehested, P.L. Hansen, B.S. Clausen, J.R. Rostrup-Nielsen, F. Abild-Pedersen, J.K. Nørskov, Atomic-scale imaging of carbon nanofibre growth, Nature 427 (6973) (2004) 426–429.

[54] S. Shoji, X. Peng, T. Imai, P.S. Murphin Kumar, K. Higuchi, Y. Yamamoto, T. Tokunaga, S. Arai, S. Ueda, A. Hashimoto, N. Tsubaki, M. Miyauchi, T. Fujita, H. Abe, Topologically immobilized catalysis centre for long-term stable carbon dioxide reforming of methane, Chem. Sci. 10 (13) (2019) 3701–3705.

[55] E. le Saché, T.R. Reina, Analysis of Dry Reforming as direct route for gas phase CO_2 conversion. The past, the present and future of catalytic DRM technologies, Prog. Energy Combust. Sci. 89 (2022), 100970.

[56] V.R. Choudhary, S. Banerjee, A.M. Rajput, Continuous production of H2 at low temperature from methane decomposition over Ni-containing catalyst followed by gasification by steam of the carbon on the catalyst in two parallel reactors operated in cyclic manner, J. Catal. 198 (2001) 136–141.

[57] H. Li, Y. Guo, J. Robertson, Calculation of TiO_2 surface and subsurface oxygen vacancy by the screened exchange functional, J. Phys. Chem. C 119 (2015) 18160–18166.

[58] S. Takenaka, Y. Tomikubo, E. Kato, K. Otsuka, Sequential production of H_2 and CO over supported Ni catalysts, Fuel 83 (2004) 47–57.

[59] K. Shibata, T. Kiyoura, J. Kitagawa, T. Sumiyoshi, K. Tanabe, Acidic properties of binary metal oxides, Bull. Chem. Soc. Jpn 46 (1973) 2985–2988.

[60] K. Arata, S. Akutagawa, K. Tanabe, I.I.I. Epoxide Rearrangement, Isomerization of 1-Methylcyclohexene Oxide over TiO_2–ZrO_2, $NiSO_4$ and $FeSO_4$, Bull. Chem. Soc. Jpn. 49 (1976) 390–393.